Large Activation Energy Barriers to Chaperone−Peptide Complex Formation and Dissociation†

Carol D. Farr, Floyd J. Galiano, and Stephan N. Witt*

Department of Biochemistry and Molecular Biology, Louisiana State University Medical Center, 1501 Kings Highway, Shreveport, Louisiana 71130-3932

Received July 24, 1995; Revised Manuscript Received September 29, 1995⊗

ABSTRACT: To probe the mechanism of chaperone substrate selection, we have investigated the kinetics of complex formation and dissociation between the molecular chaperone DnaK and a short peptide (Cro, representing amino acids 1−12 of the cro repressor protein). The Cro peptide was N-terminally labeled with the environmentally sensitive fluorophore dansyl chloride (Cro*), and steady-state and stopped-flow fluorescence spectroscopies and fluorescence-detected high-performance size exclusion chromatography (HPSEC) were used to monitor complex formation and dissociation over a range of temperatures in the absence of ATP. The results are summarized as follows: (i) Cro* binds to DnaK with a second-order rate constant, k_{on}, which varies from 8 to 200 M^{-1} s^{-1} between 15 and 37 °C. The slow on-rate is a consequence of a large activation energy barrier. The activation enthalpy (ΔH^*) and the prefactor [ω exp($\Delta S^*/R$)] are 26 kcal mol^{-1} and 7 × 10^{20} M^{-1} s^{-1}, respectively. (ii) Once formed, DnaK−Cro* complexes are long-lived, especially at low temperatures (T < 15 °C). The off-rate is unusually temperature-sensitive, for example, there is a *478-fold increase* in k_{off} from 2.3 × 10^{-6} to 1.1 × 10^{-3} s^{-1} over a range of only 30 °C (5−35 °C). The steep temperature-dependence of the off-rate is a consequence of a very large activation energy barrier to DnaK−Cro* complex dissociation [ΔH^* = 34.6 kcal mol^{-1} and ω exp($\Delta S^*/R$) = 2 × 10^{21} s^{-1}]. The relatively low affinity of the Cro* peptide for DnaK is due to a large kinetic barrier to *binding*. We discuss possible causes for these large kinetic barriers.

The 70-kDa class of molecular chaperones utilizes free energy from ATP[1] binding and hydrolysis to mediate "housekeeping" activities that are common to all cells, such as protein folding and transport and protein assembly and disassembly [for reviews see Gething and Sambrook (1992), Georgopoulos and Welch (1993), Hendrick and Hartl (1993), Becker and Craig (1994)]. The common element among these diverse activities is the transient and selective binding of the chaperone to accessible sites on substrate proteins. While nearly all organisms express highly homologous constitutive and stress-inducible chaperones, and despite their importance for maintaining a cell's metabolic machinery, little is known about the kinetics and mechanism of substrate binding by the 70-kDa class of molecular chaperones.

A 70-kDa chaperone consists of two functional domains: the N-terminal (44-kDa) domain contains the nucleotide binding site, and the C-terminal (23-kDa) domain contains the substrate binding site. The three-dimensional structure of the N-terminal domain is similar to the nucleotide binding site of hexokinase (Flaherty et al., 1990). The three-dimensional structure of the C-terminal domain is not known, however. On the basis of similarities in the sequences of class I MHC molecules and members of the 70-kDa family of chaperones, the structure of the peptide binding site of class I MHC proteins has been used to model the structure of the C-terminal domain of molecular chaperones (Rippmann et al., 1991). We note that preliminary NMR evidence from a study (Zuiderweg et al., 1995) on a genetically engineered truncated version of the peptide binding site from a 70-kDa chaperone (heat shock cognate protein) indicates that the site contains a preponderance of β-sheet. The two functional domains are conformationally coupled, that is, the binding of Mg-ATP and potassium ions to the N-terminal domain triggers the release of bound substrates (Palleros et al., 1993a). Conversely, substrate binding triggers the hydrolysis of adenosine triphosphate (Flynn et al., 1989).

Peptides have been used to probe various aspects of chaperone chemistry. For example, combinatorial peptide libraries have been used to probe the substrate specificity of the chaperones BiP and DnaK (Flynn et al., 1991; Blond-Elguindi et al., 1993; Gragerov et al., 1994). DnaK, the chaperone used in this study, is expressed by *Escherichia coli* and selects for peptides that contain a hydrophobic core that is flanked near the N- and C-termini by positively charged residues (Gragerov et al., 1994); negatively charged residues within the peptide appear to reduce or even eliminate binding. Schmid and co-workers (1994) recently investigated the pre-steady-state kinetics of the binding reaction of the 21-mer targeting signal prepiece of the precursor of mitochondrial aspartate aminotransferase (pp-1) to DnaK (Table 1). The pp-1 peptide, which contains two hydrophobic cores flanked by positively charged residues, binds and dissociates relatively rapidly at 25 °C in the absence of adenosine triphosphate (k_{on} = 9400 M^{-1} s^{-1} and k_{off} = 4 × 10^{-3} s^{-1}). ATP significantly lowers the affinity of pp-1 for DnaK by differentially increasing the on- and off-rates (k_{on} = 3.5 ×

†Support for this work came in part from the NIH (GM51521-02).

* Address correspondence to Stephan N. Witt. Tel.: (318) 675-7891. FAX: (318) 675-5180. E-mail:SWITT1@NOMVS.LSUMC.EDU.

⊗ Abstract published in *Advance ACS Abstracts,* November 15, 1995.

[1] Abbreviations: ATP, adenosine triphosphate; BSA, bovine serum albumin; CA, carbonic anhydrase; HPLC, high-performance liquid chromatography; HPSEC, high-performance size exclusion chromatography; LB, Luria broth; 2-ME, 2-mercaptoethanol; NMR, nuclear magnetic resonance.

0006-2960/95/0434-15574$09.00/0

Table 1: Sequences of Peptides Used and/or Discussed in this Study

peptide sequence		ref
−+ +− MQERITLKDYAM	(Cro)	Sherman & Goldberg, 1991; Gragerov et al., 1994
+ + + KLIGVLSSLFRPK	(VSV13)	Flynn et al., 1989; Landry et al., 1992
+ + LFRPK	(VSV5)	
+ ++ + CALLQSRLLLSAPRRAAATARA	(pp-1)	Schmid et al., 1994

10^5 M^{-1} s^{-1} and k_{off} = 1.5 s^{-1}). In general, ATP binding and hydrolysis modulates chaperone activity (Palleros et al., 1993; Schmid et al., 1994). In *E. coli*, the cochaperones GrpE and DnaJ also function to modulate the activity of DnaK (Wall et al., 1995).

Since the activity cycle of a molecular chaperone occurs on a relatively short time scale (seconds to minutes), chaperone substrate selection is most likely a predominantly *kinetic* rather than an equilibrium phenomenon (see Appendix). We are interested in how the composition of a peptide affects the kinetics of chaperone−peptide complex formation and dissociation. The Cro peptide, with known reactivity for DnaK (Sherman & Goldberg, 1991; Gragerov et al., 1994), was chosen for this detailed kinetic study because it possesses a relatively polar sequence (Table 1) in contrast to the paradigmatic hydrophobic peptide, which DnaK selects from combinatorial peptide libraries, as stated above. Here we show that there are unusually large kinetic barriers to DnaK−Cro* complex formation and dissociation in the absence of adenosine triphosphate. The relatively low-affinity binding of Cro to DnaK is a consequence of a large kinetic barrier to binding ($K_d = k_{off}/k_{on} = 1.3 \times 10^{-4}$ $s^{-1}/18$ M^{-1} $s^{-1} = 7$ μM). We suggest that two negatively charged residues within the Cro peptide retard the rate of binding.

MATERIALS AND METHODS

Cell Culture. DnaK was harvested from the *E. coli* strain RLM893 (Zylicz & Georgopoulos, 1984). Cells were incubated in standard Luria broth (LB) media supplemented with 0.4% glucose and 25 μg of chloramphenicol/mL. Cells were first cultured at 30 °C to mid-log phase, diluted into fresh LB media, incubated an additional hour at 30 °C, and then shifted to 37 °C and incubated until late-log phase (4−6 h).

DnaK Purification. DnaK purification followed the procedures of Cegielska and Georgopoulos (1989) with minor modifications. Unless stated otherwise, all reagents were of the highest purity and were purchased from Sigma. The purification steps preceding the MONO Q column took place at 0 °C. Briefly, approximately 30 g of cells, suspended in 10% sucrose/50 mM Tris at pH 8.0, were sonicated on ice for five 1-min treatments, and then the cell suspension was incubated for 30 min with lysozyme (2 mg/mL). After centrifugation to pellet cellular debris, proteins in the supernatant were precipitated with ammonium sulfate (65% saturation). Following additional centrifugation, the resuspended pellets were passed over an ATP-agarose column (Sigma A2767) equilibrated in 25 mM HEPES/10 mM KCl/3 mM $MgCl_2$/1 mM EDTA/5 mM 2-mercaptoethanol (2-ME) at pH = 8.0. The ATP column was eluted with 6 mM ATP/$MgCl_2$. Fractions were pooled, and then DnaK was preciptated with ammonium sulfate (70% saturation). The resuspended pellets were then dialyzed overnight against 3 L of the MONO Q buffer (25 mM TRIS/50 mM KCl/1 mM EDTA/5 mM 2-ME at pH = 7.8). DnaK was eluted from the MONO Q column (Pharmacia, HR 5/5) with a 50−500 mM KCl gradient at room temperature, as described by Walker and McCarty (1991). Fractions were assayed by SDS−PA gel electrophoresis to determine which fractions contained DnaK. Fractions containing DnaK were pooled and dialyzed for 48−72 h against 8−12 L of the sample buffer (25 mM HEPES/50 mM KCl/5 mM $MgCl_2$/5 mM 2-ME at pH = 7.0). DnaK, purified as described above, appears as a single band on a Coomassie Blue-stained SDS−PA gel; densitometric scans of such gels give an estimate of DnaK purity at >98%. Protein concentrations were determined by the Bio-Rad protein assay.

DnaK used in ATPase assays was put through an additional purification step. To remove small amounts of contaminating ATPases, DnaK was passed over a size exclusion column (see below) (Palleros et al., 1993b). The fraction containing DnaK was collected and then concentrated using a Centricon-30 microconcentrator (Amicon).

Peptides and Fluorophores. Peptides, synthesized using 9-fluorenylmethyloxycarbonyl (FMOC) chemistry, were purchased from the University of Kentucky's Core Facility. Dansyl chloride was purchased from Molecular Probes. The sequences of the peptides that were used in this study are shown in Table 1. The Cro peptide represents amino acids 1−12 of the cro repressor protein, which is expressed by bacteriophage λ (Hsiang et al., 1977). As discussed below, two control peptides were used in this study: VSV13 represents amino acids 490−502 of the New Jersey strain of vesicular stomatitis virus glycoprotein (Gallione & Rose, 1983), and VSV5 represents amino acids 498−502 of the New Jersey strain of vesicular stomatitis virus glycoprotein. The dansylation of the Cro peptide was accomplished using peptide-bound resin so that all reactive groups, except the N-terminal amine, were blocked with protecting groups. The labeling reaction consisted of approximately 0.1 g of peptide-bound resin suspended in 5 mL of dimethyl formamide containing a 3-fold molar excess (over peptide) of diisopropyl ethanol amine and a 2-fold molar excess of dansyl chloride. The reaction was stopped after 1.5 h of shaking, and the resin was washed and dried. Peptides were cleaved and deprotected with an N_2-purged cocktail of 85% TFA, 5% anisole, 5% thioanisole, and 5% 1,2-ethanedithiol. Peptides were purified via high-performance liquid chromatography (HPLC) using a reverse phase C_4 column (Vydac, #214TP1010). Electrospray ion mass spectroscopy was used to verify peptide identity (Louisiana State University, New Orleans, Core Facility). Concentrations of dansylated peptide solutions were determined by measuring the absorbance of the dansyl group (ϵ_{335} = 4600 M^{-1} cm^{-1}; Haugland, 1992). Concentrations of unlabeled Cro peptide solutions were determined by measuring the absorbance of tyrosine (ϵ_{275} = 1450 M^{-1} cm^{-1}; Brandts & Kaplan, 1973). Concentrations of unlabeled VSV13 solutions were determined via quantitative amino acid analysis (University of Kentucky Core Facility). The dansyl label is denoted as an asterisk (*).

ATPase Assay. ATPase assays were carried out as outlined by Haber and Walker (1991). The assay mixture

was composed of the following reagents: 25 μL of the reaction buffer (60 mM TRIS/1.5 mM $CaCl_2$/1.5 mM $MgCl_2$/3 mM dithiothreitol/0.3 mM EDTA at pH = 7.6); 30 μL of 3 μM DnaK in the sample buffer (25 mM HEPES/50 mM KCl/5 mM $MgCl_2$/5 mM 2-ME at pH = 7.0); 4.5 μL of concentrated peptide in the sample buffer; 13.4 μL (13.4 μCi) of [2,8-^{3}H]ATP (36 Ci/mmol) in 1:1 ethanol:water (NEN, 1 Ci = 3.7×10^{10} Bq); and 2.25 μL of 500 mM ATP in water. The ATPase reactions were carried out at 37 °C. Aliquots (6 μL) were periodically removed and mixed with a stop solution (2 μL) (50 mM EDTA/4 mM ATP/4 mM ADP). Aliquots of the stopped reactions were spotted on PEI-cellulose plates (Baker) and developed as described (Haber & Walker, 1991). The spots on the PEI-cellulose plates corresponding to ATP and ADP were identified with a UV-lamp and scraped into scintillation vials, and then the radioactivity was counted. Liquid scintillant was purchased from DuPont. At 37 °C DnaK hydrolyzes ATP at a rate of 0.082 ± 0.005 min^{-1}. This turnover number (k_{cat}) agrees with a previously reported value for highly pure DnaK (Palleros et al., 1993b).

Sample Preparation. Preformed DnaK−Cro* complexes were prepared as follows. DnaK (4.0 μM) was incubated with Cro* (10 μM) for 60−90 min at 37 °C. DnaK−Cro* complexes were then separated from the excess free Cro* via passage over the HPSEC column, and the fraction containing DnaK−Cro* complexes was collected and stored at 0 °C until ready for use. At time zero, excess unlabeled Cro (20 μM) was added to inhibit rebinding (Cro* + DnaK → DnaK−Cro*). Samples for the peptide inhibition experiments had a fixed concentration of Cro* with varying concentrations of unlabeled peptides. Samples were incubated in a heater/cooler bath (Fisher Scientific, model 9101), which maintained the temperature to ±0.1 °C.

Analytical Ultracentrifugation. A Beckman XL-A ultracentrifuge in the Department of Chemistry, Louisiana State University, Baton Rouge, LA, was used in the sedimentation equilibrium experiments on the unlabeled and labeled Cro peptides. The samples (in 25 mM HEPES and 50 mM KCl at pH = 7.0) were spun for approximately 18 h at 40 000 rpm at 25 °C. The detection wavelengths were 275 and 335 nm. The sedimentation equilibrium data were analyzed using eq 1 (McRorie & Voelker, 1993), where $c(r)$ is the concentration at radius r, c_{r_o} is the concentration of the monomer at the reference radius r_o, ω is the angular velocity, R is the gas constant, T is the temperature in Kelvin, M is the molecular weight, ν is the partial specific volume of the solute (peptide), and ρ is the density of the solvent. The partial specific volume of the Cro* peptide ($\nu_{Cro*} = 0.72$ mL g^{-1}) was calculated using standard values for the partial specific volumes of amino acid residues (Zamyathin, 1984). The solvent density ($\rho = 0.998$ g mL^{-1}) was determined experimentally.

$$c(r) = c_{r_o} \exp\{[\omega^2 M(1 - \nu\rho)(r^2 - r_o^2)]/2RT\} \quad (1)$$

High-Performance Size Exclusion Chromatography. A Bio-Rad size exclusion column (Bio-Sil SEC-250, 300 × 7.8 mm) with a precolumn (100 × 7.8 mm) was connected to a Gilson two-pump HPLC system. The column run-through passed through a UV−vis detector (Gilson, model 218) and a fluorescence detector (Gilson, model 121) in series. The UV−vis detector was set at 280 nm. The fluorescence detector was equipped with a 310−410 nm excitation filter and a 510−650 nm emission filter. The column experiments were conducted with a mobile phase of 25 mM KH_2PO_4−K_2HPO_4/50 mM KCl/5 mM 2-ME (pH = 7.0) at room temperature with a flow rate of 0.75 mL/min. Bovine serum albumin (BSA) and carbonic anhydrase (CA) were used as molecular weight standards. The elution volumes of DnaK, BSA, CA, and Cro* were 12.5, 13.1, 16.2, and 26.5 mL, respectively.

Fluorescence Instrumentation. A SLM SPF-500 C spectrofluorometer was used for the steady-state fluorescence experiments. The sample holder was thermostated to the desired temperature via an external water bath. Temperature was maintained to ±0.5 °C. The excitation wavelength was 335 nm, which is the wavelength of maximal absorption by the dansyl group. Excitation and emission slits were set at 5 nm.

An Applied Photophysics stopped-flow spectrometer (DX-17MV) with fluorescence detection was used for experiments conducted at 37 °C. An Oriel 470 nm long-pass filter was used to remove stray excitation radiation ($\lambda_{ex} = 335$ nm).

Analysis of the Complex Formation Kinetic Curves. The kinetics of DnaK−Cro* complex formation and dissociation are consistent with reversible reaction 2 in which Cro* and DnaK−Cro* denote the free fluorescent peptide and bound fluorescent peptide with enhanced emission, respectively. For complex formation reactions carried out with [DnaK] > [Cro*], the experimental formation traces followed single-exponential kinetics according to eq 3

$$\text{Cro*} + \text{DnaK} \underset{k_{off}}{\overset{k_{on}}{\leftrightarrow}} \text{DnaK−Cro*} \quad (2)$$

$$F(t) = F_{eq}[1 - \exp(-k_{obs}t)] \quad (3)$$

where F_{eq} is the fluorescence intensity of the stable asymptote at long times, and k_{obs} is the observed first-order rate constant. The formation curves were fitted to eq 3 to obtain values for k_{obs}. The observed rate constant is related to the second-order rate constant for peptide binding (k_{on}) and the first-order rate constant for peptide dissociation (k_{off}) by eq 4.

$$k_{obs} = k_{on}[\text{DnaK}] + k_{off} \quad (4)$$

The numerical values for k_{on} and k_{off} reported here were obtained from the slope and y-intercept of the least squares fit of the observed rate constants to eq 4. The uncertainties in the rate constants were determined according to Bevington (1969).

RESULTS

Since a dansylated Cro peptide (Cro*) was used throughout this kinetic study, several experiments were conducted to ascertain whether specific N-terminal dansylation altered the physical and/or the biological properties of the Cro peptide. As part of the characterization of the unlabeled and labeled Cro peptides, two control peptides (Table 1) were used. The VSV13 peptide, which is known to bind to DnaK (Landry et al., 1992) and to the chaperone BiP (Flynn et al., 1989), was used as a positive control. The VSV5 peptide, which exhibits only negligible binding to DnaK, was used as a negative control.

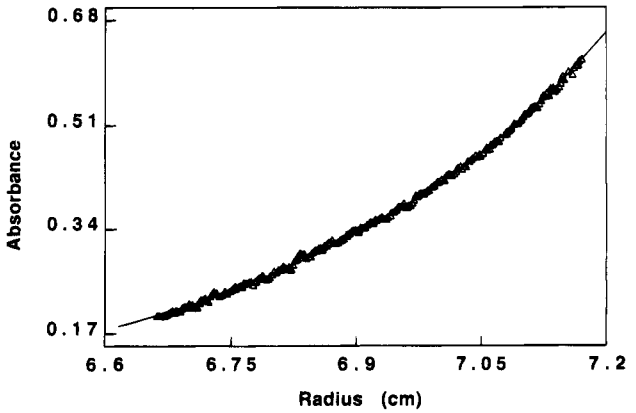

FIGURE 1: Sedimentation equilibrium analysis of the dansylated Cro peptide. A plot of the absorbance at 335 nm versus the radial distance. The solid line is the theoretical sedimentation curve for a Cro* monomer; the open triangles represent the data points. The theoretical curve was calculated from the eq 1 with the following parameters: $c_{r_0} = 60\ \mu M$; $\rho = 0.998$ g mL^{-1}; $\nu_{Cro*} = 0.72$ mL g^{-1}; M = 1732 g mol^{-1}; $\omega = 40\,000$ rpm; $T = 298$ K; and $R = 8.314 \times 10^7$ erg mol^{-1} K^{-1}.

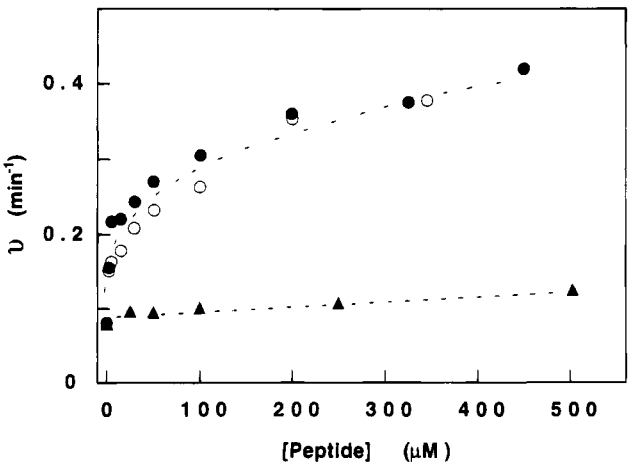

FIGURE 2: The rate of DnaK-catalyzed ATP hydrolysis versus peptide concentration. Closed circles represent the unlabeled Cro peptide; open circles represent the dansylated Cro peptide; and closed triangles represent the unlabeled VSV5 peptide. The dotted lines are to help guide the eye (temperature = 37 °C).

Analytic Ultracentrifugation. To avoid artifacts due to peptide aggregation, the solution molecular weights of the unlabeled and labeled Cro peptides were determined using analytic ultracentrifugation. The results obtained from a sedimentation equilibrium experiment on the Cro* peptide (60 μM) at 25 °C are shown in Figure 1. The absorbance of the Cro* peptide at 335 nm as a function of the radial distance from the center of the rotor is consistent with the theoretical molecular weight of monomeric Cro* (M = 1732 g mol^{-1}). The unlabeled Cro peptide also sediments as a monomer at 25 °C, even at an initial concentration of 200 μM (data not shown). Since the Cro* peptide is monomeric at relatively high concentrations, the peptide is certainly monomeric at the low concentrations (~0.5 μM) used in the kinetic experiments in this study.

ATPase Assay. We assessed whether N-terminal dansylation of the Cro peptide alters its ability to stimulate the ATPase activity of DnaK. Over a wide range of peptide concentrations (1−450 μM) (Figure 2), unlabeled and labeled Cro stimulate the ATPase activity of DnaK to nearly the same magnitude. Maximal stimulation occurs for both peptides at ~400−500 μM, with $\nu_{ATP} = 0.4$ min^{-1}. The K_M for unlabeled Cro is approximately 30 μM at 37 °C, confirming the results of Gragerov et al. (1994); we found the K_M for labeled Cro to be nearly identical.

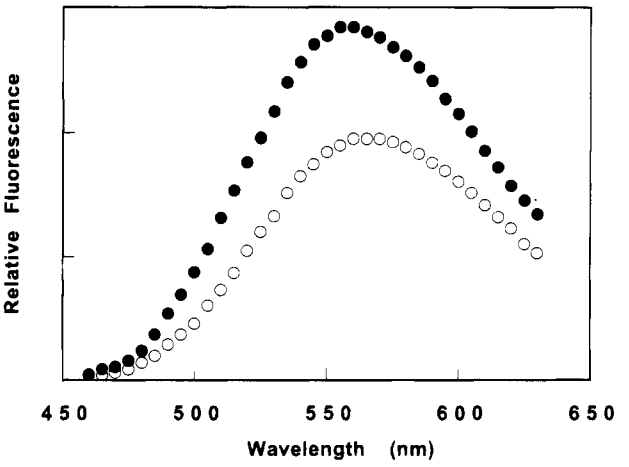

FIGURE 3: Effect of DnaK on the fluorescence spectrum of the dansylated Cro peptide. Closed and open squares trace the fluorescence spectra of the dansylated Cro peptide in the presence and absence of DnaK, respectively. Conditions: [Cro*] = 0.34 μM; [DnaK] = 6.0 μM; temperature = 25 °C; $\lambda_{ex} = 335$ nm.

To demonstrate that the observed increase in ATPase activity of DnaK is a consequence of specific peptide binding, the stimulatory ability of a 5-mer peptide (VSV5) was assessed. As expected, unlabeled VSV5 causes only a negligible stimulation of the ATPase activity of DnaK over a wide concentration range. On the basis of the combined results from the analytic ultracentrifugation experiments and the ATPase assays, we conclude that the dansylated Cro peptide is monomeric, and N-terminal dansylation does not alter the stimulatory ability of the peptide.

Effect of DnaK on the Fluorescence Spectrum of Cro.* The fluorescence spectra of the Cro* peptide (0.34 μM) in the absence and presence of added DnaK (6.3 μM) at 25 °C are shown in Figure 3. In the absence of added DnaK, the fluorescence spectrum of the Cro* peptide is a broad band centered at $\lambda_{max} = 565$ nm. Two spectral changes occurred following the incubation of the Cro* peptide with excess DnaK for 1 h. There was a 47% increase in the total fluorescence and a 10 nm blue-shift of the fluorescence maximum from 565 to 555 nm. To ensure that the observed fluorescence enhancement was not due to nonspecific binding of the dansyl moiety to DnaK, in separate experiments excess DnaK was incubated with the dansylated VSV5 peptide. Only a slight increase in dansyl fluorescence occurred in this negative control (data not shown). Thus the observed increase in dansyl fluorescence and the spectral blue-shift, which occur upon addition of DnaK to the dansylated Cro peptide, are consistent with reversible complex formation according to reaction 2.

Isolation of DnaK−Cro Complexes via HPSEC.* DnaK−Cro* complex formation was verified using fluorescence- and absorbance-detected HPSEC. In this column assay, DnaK−Cro* complexes are separated from free Cro* peptide. DnaK (4 μM) and Cro* (10 μM) were incubated for 60 min at 37 °C to form complexes. Upon injection of an aliquot onto the HPSEC column, two main bands ($V_e = 12.5$ and 26.5 mL) are observed in the fluorescence-detected chromatogram (Figure 4). Separate injections of DnaK

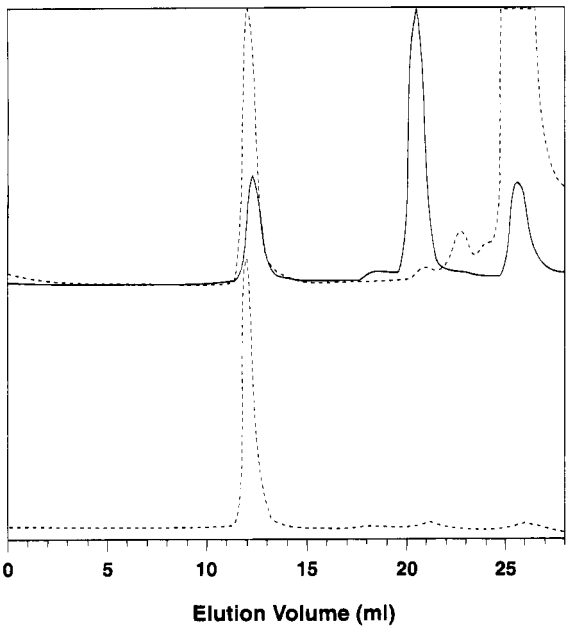

FIGURE 4: Isolation of long-lived DnaK−Cro* complexes by size exclusion chromatography. Top panel: DnaK (4.0 μM) was incubated with Cro* (10 μM) for 60 min at 37 °C and then injected on the HPSEC column (absorbance, solid line; fluorescence, dotted line). Bottom panel: The fraction at 12.5 mL, which is due to DnaK−Cro* complexes, was collected and reinjected (fluorescence, dotted line).

(absorbance detection) and Cro* (fluorescence detection) enabled us to assign these two bands to the DnaK−Cro* complex and free Cro* (data not shown), respectively. We note that DnaK elutes as a monomer even at fairly high concentrations (6 μM), which is consistent with the results from several other labs (Schmid et al., 1986; Palleros et al., 1991). The band at 21 mL in the absorbance-detected chromatogram has variable intensity and is not due to protein. The fraction at 12.5 mL was collected, stored on ice, and then reinjected 1 h later. Upon reinjection, a band is observed in the fluorescence-detected chromatogram at the same position (Figure 4). The above results reveal that DnaK−Cro* complexes are surprisingly long-lived.

Specificity controls were conducted using the fluorescence-detected HPSEC column assay to determine whether unlabeled peptides inhibit Cro* binding to DnaK. A 50% inhibition is attained when [Cro]/[Cro*] = 3, instead of at the expected ratio of 1:1 (Figure 5). This result indicates that Cro* binds to DnaK with a slightly higher affinity than unlabeled Cro. As expected, DnaK−Cro* complex formation is completely inhibited at a large ratio of unlabeled to labeled Cro*. The unlabeled VSV13 peptide also inhibits Cro* binding to DnaK (Figure 5). On the basis of these results we conclude that (i) DnaK−Cro* complex formation is specific; (ii) the Cro peptide and the VSV13 peptide have similar affinities for DnaK; and (iii) the Cro peptide and the VSV13 peptide bind at the same site on DnaK.

Formation Kinetics. The kinetics of reversible DnaK−Cro* complex formation (reaction 2), in the absence of ATP, were investigated over a limited temperature range (15−37 °C). Complex formation was followed by monitoring the increase in dansyl fluorescence upon Cro* binding to DnaK (Figure 3). Complex formation proceeds so slowly between 15 and 25 °C that the reactions were conveniently monitored using a steady-state fluorescence instrument. At 37 °C,

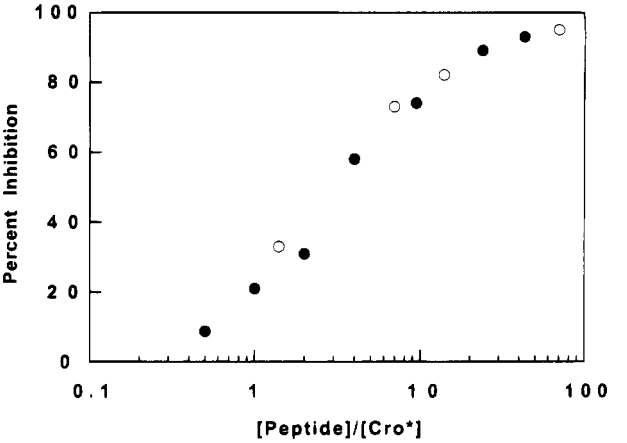

FIGURE 5: Inhibition of DnaK−Cro* complex formation by unlabeled peptides. DnaK (1.0 μM) was co-incubated with Cro* (4.2 μM) and varying amounts of either unlabeled Cro or unlabeled VSV13. Closed circles, Cro; open circles, VSV13 (T = 37 °C).

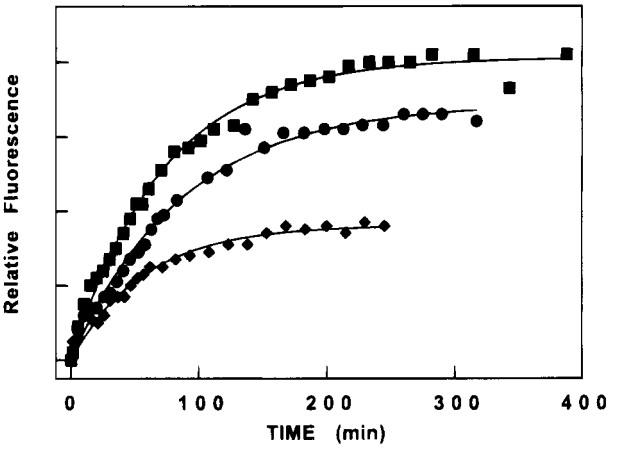

FIGURE 6: Kinetics of DnaK−Cro* complex formation at 25 °C. Complex formation was followed using steady-state spectroscopy. [Cro*] = 0.35 μM. Closed diamonds, [DnaK] = 0.7 μM; closed circles, [DnaK] = 1.8 μM, and closed squares, [DnaK] = 4.3 μM. λ_{ex} = 335 nm and λ_{em} = 560 nm. Data sets were fitted to a single-exponential function (solid lines).

complex formation was monitored using a stopped-flow fluorescence instrument set on a long time-base (17 min).

DnaK−Cro* complex formation traces, which were obtained at 25 °C, are shown in Figure 6. For each kinetic experiment, the Cro* concentration was fixed at 0.35 μM while the DnaK concentration was varied from 0.7 to 6.3 μM. As the DnaK concentration is increased, there is a parallel increase in the rates of complex formation and the values of the stable asymptotes at long times, as expected. Each formation trace was fitted to a single-exponential function to obtain a value for k_{obs}. The plot of k_{obs} versus [DnaK] is linear with a slope and y-intercept equal to 18 M^{-1} s^{-1} and 1.3 × 10^{-4} s^{-1} (Figure 7), respectively. [DnaK−Cro* complex formation at 25 °C was also followed using fluorescence-detected HPSEC in experiments where peptide was varied (1.5−10 μM) while the concentration of DnaK was fixed (0.15 μM) (data not shown). The k_{on} and k_{off} values, obtained from a plot of k_{obs} versus [Cro*], were 20 M^{-1} s^{-1} and 2.8 × 10^{-4} s^{-1}, respectively.] The kinetic traces from experiments conducted at 15 and 37 °C were analyzed in a similar way (data not shown). The rate constants are given in Table 2. Activation parameters for complex formation are calculated below.

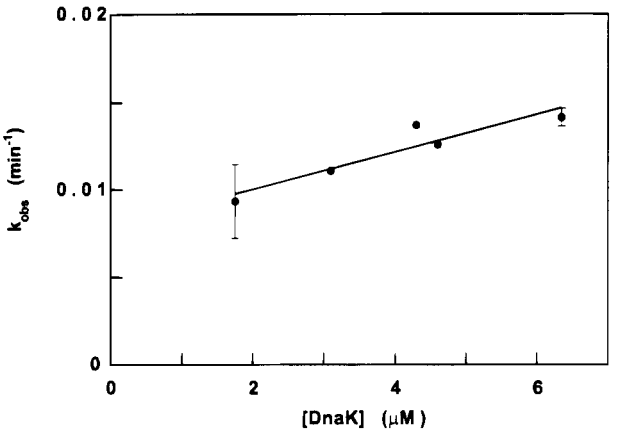

FIGURE 7: Plot of k_{obs} versus [DnaK]. The k_{obs} values were obtained by fitting the 25 °C experimental formation traces (Figure 6) to a single-exponential function. The solid line was obtained from a least-squares fit of the data to the equation for a straight line. The slope and y-intercept of the plot equal 18 M^{-1} s^{-1} and 1.3 × 10^{-4} s^{-1}, respectively.

Table 2: On- and Off-Rate Constants as a Function of Temperature

	complex formation experiments[a]		complex dissociation experiments[b]
temperature (°C)	k_{on} (M^{-1} s^{-1})	k_{off} (s^{-1})	k_{off} (s^{-1})
5			2.3 ± 0.2 × 10^{-6}
15	8 ± 4	6.0 ± 2.0 × 10^{-5}	2.0 ± 0.1 × 10^{-5}
25	18 ± 5	1.3 ± 0.2 × 10^{-4}	1.2 ± 0.2 × 10^{-4}
35			1.1 ± 0.2 × 10^{-3}
37	200 ± 124	3.4 ± 0.3 × 10^{-3}	

[a] On- and off-rate constants were determined from plots of k_{obs} versus [DnaK]. The uncertainties in the rate constants were calculated according to Bevington (1969). [b] Off-rate constants determined from complex dissociation experiments. The uncertainties in the off-rate constants represent the standard errors of the mean of either duplicate or triplicate determinations.

Dissociation Kinetics. The kinetics of Cro* dissociation from preformed DnaK−Cro* complexes (reverse reaction 2) were investigated over a range of temperatures using fluorescence-detected HPSEC to directly determine off-rate constants. Preformed DnaK−Cro* complexes were prepared as described. Samples were incubated at the desired temperature, and aliquots were removed at various times and injected on the HPSEC column. The integrated intensity of the band at 12.5 mL, which is proportional to the number of DnaK−Cro* complexes, was determined for each injection. The DnaK−Cro* molecular complex dissociation curves in Figure 8 represent the integrated intensity of the band at 12.5 mL at time t divided by the integrated intensity of the first injection [$I(t)/I(t=0)$]. Cro* peptide dissociation from preformed DnaK−Cro* complexes follows first-order kinetics at each temperature we investigated (5−35 °C). The effect of temperature on the half-time ($t_{1/2}$ = [ln 2]/k_{off}) for Cro* peptide dissociation is remarkable. There is *478-fold decrease* in $t_{1/2}$ from 84 to 0.18 h when the temperature is increased by only 30 °C. Significantly, the k_{off} values obtained from the HPSEC experiments are nearly identical to k_{off} values obtained from the complex formation experiments (Table 2).

Arrhenius plots of the on- and off-rate constants in Table 2 are shown in Figure 9. The activation enthalpy (ΔH^*) and the prefactor [ω exp($\Delta S^*/R$)] are obtained from the slope

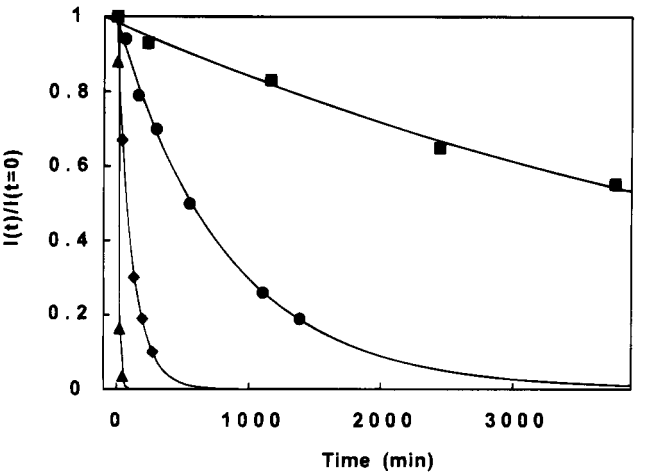

FIGURE 8: Kinetics of Cro* dissociation from preformed DnaK−Cro* complexes (5−35 °C). Dissociation kinetics were monitored by fluorescence-detected SEC. The approximate concentration of DnaK−Cro* complexes was 0.4 μM. Each sample contained 20 μM unlabeled Cro. Closed squares, 5 °C; closed circles, 15 °C; closed diamonds, 25 °C; and closed triangles, 35 °C. Each data set was fitted to a single-exponential function (solid lines).

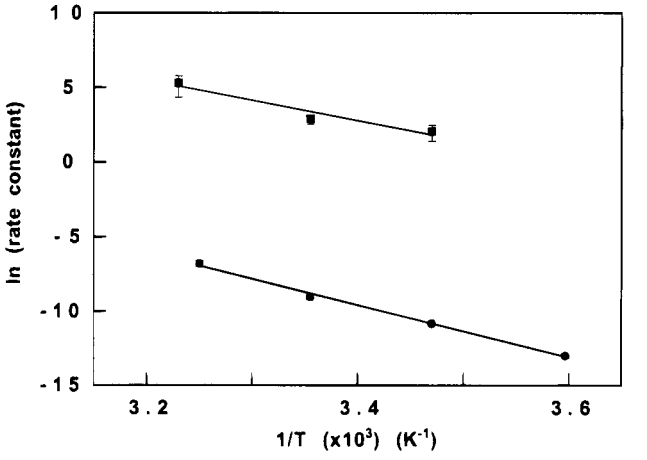

FIGURE 9: Arrhenius temperature-dependence of the on- and off-rate constants. Plots of ln k_{on} and ln k_{off} versus $1/T$. The activation enthalpy and prefactor for Cro* peptide binding to DnaK (closed squares) are 26 ± 8 kcal/mol and 7 × $10^{20\pm 6}$ M^{-1} s^{-1}. The activation enthalpy and prefactor for Cro* peptide dissociation from DnaK (closed circles) are respectively 34.6 ± 1.2 kcal/mol and 2 × $10^{21\pm 1}$ s^{-1}. Solid lines represent the least-squares fit of the data to the equation ln k = ln ω + $\Delta S^*/R$ − $\Delta H^*/RT$.

and intercept of each plot, respectively. The activation parameters for Cro* peptide binding to DnaK (upper plot) are ΔH^* = 26 ± 8 kcal mol^{-1} and ω exp($\Delta S^*/R$) = 7 × $10^{20\pm 6}$ M^{-1} s^{-1}. The activation parameters for Cro* peptide dissociation from DnaK (lower plot) are ΔH^* = 34.6 ± 1.2 kcal mol^{-1} and ω exp($\Delta S^*/R$) = 2 × $10^{21\pm 1}$ s^{-1}.

DISCUSSION

In this report, we have determined that there are very large activation energy barriers to complex formation and dissociation between the molecular chaperone DnaK and a N-terminally dansylated dodecameric peptide (Cro*). Because of the unexpectedly slow rate of Cro* binding to DnaK, several control experiments were executed to ensure that the kinetic experiments were free of artifacts. To that end we have determined that the N-terminally dansylated Cro peptide is monomeric (Figure 1); the dansyl label does not signifi-

cantly alter the affinity of the Cro peptide for DnaK (Figures 2 and 5); and Cro* binding to DnaK is specific (Figures 2, 3, and 5) and follows reaction 2. Possible causes for these large activation energy barriers are discussed below.

The Cro* peptide binds to DnaK with slow second-order kinetics (k_{on} = 8−200 M^{-1} s^{-1}) (Table 2). The relaxation time to reach equilibrium is approximately 80 mins at 25 °C at micromolar concentrations of protein and peptide (Figure 6). This slow binding is a consequence of a large activation enthalpy (ΔH^* = 26.0 kcal mol^{-1}) (Figure 9). One explanation for this large ΔH^* value is that substantial electrostatic repulsions between charged residues on the Cro* peptide and similarly charged residues in the chaperone binding site destabilize the chaperone−peptide transition state. This explanation is discussed in more detail below. Another explanation for this large ΔH^* value is that the Cro* peptide is highly solvated, and bound water must be stripped from the peptide prior to binding. The large magnitude of the prefactor (7×10^{20} M^{-1} s^{-1}) is also consistent with desolvation of the Cro* peptide prior to binding. More experiments are required in order to distinguish between these two explanations. A peptide (or any other chaperone substrate) with such a large kinetic barrier to binding would be effectively excluded from binding to a chaperone at short times ($t \approx 5$ min) especially in the presence of other substrates with more rapid on-rates (see Appendix).

DnaK−Cro* complex dissociation kinetics are intriguing because of the unusual temperature-dependence of the off-rate. Over a range of only 30 °C (5−35 °C), there is a *478-fold increase* in k_{off} from 2.3×10^{-6} to 1.1×10^{-3} s^{-1} (Figure 8, Table 2). Typically, a reaction rate doubles for every 10 °C increase in temperature (Espenson, 1981), thus only a ~10-fold increase in off-rate is expected over 30 °C. The steep temperature-dependence of the rate of DnaK−Cro* dissociation is a consequence of the very large magnitude of the activation enthalpy (ΔH^* = 34.6 kcal mol^{-1}), which indicates that a significant amount of bond breaking is required to reach the transition state. With respect to the prefactor (2×10^{21} s^{-1}), if $\omega = k_B T/h$ (k_B and h are the Boltzmann and Planck constants, respectively), then ΔS^* = 38 cal mol^{-1} K^{-1}. Such a large positive ΔS^* value indicates that a large order-to-disorder transition occurs upon dissociation of the Cro* peptide. The large magnitudes of both ΔH^* and ΔS^* are consistent with a substantial number of contacts, such as hydrogen bonds and/or hydrophobic interactions, between the Cro* peptide and the residues within the DnaK binding site. It is important to note that, using 2-D NMR techniques, Landry and co-workers (1992) determined that the VSV13 peptide is bound to DnaK in an extended conformation, cemented in place by a network of bonds between the main chain atoms of the peptide and the residues within the binding site. Although we cannot make any statements regarding the structure of the DnaK-bound Cro* peptide, since VSV13 inhibits Cro* binding, the two peptides probably bind at the same site and are thus subject to similar bonding interactions. Elsewhere we will report the kinetics of DnaK−VSV13 complex formation and dissociation (manuscript in preparation).

McCarty and Walker (1991) discovered that the rates of DnaK-catalyzed autophosphorylation and adenosine triphosphate hydrolysis exhibit a steep temperature-dependence. DnaK's ATPase and autophosphoylation activities increase 70- and 400-fold, respectively, between 20 and 50 °C at pH 6.2. On the basis of their results, they proposed that such large responses to only small changes in temperature are consistent with DnaK functioning as a temperature sensor: a molecular thermometer. Using the data in the Arrhenius plot in Figure 6 to extrapolate to 50 °C, we calculate a 250-fold increase in the rate of DnaK−Cro* complex dissociation between 20 and 50 °C. Although such a steep temperature-dependence of the Cro* off-rate is consistent with the idea that DnaK is a molecular thermometer, clearly more work is required to see whether other DnaK−peptide complexes exhibit such a temperature-sensitive off-rate.

It is useful to compare the Cro* on- and off-kinetic results reported here to the recent results of Schmid and co-workers (Schmid et al., 1994). In this comparison, we assume the Cro* peptide and the pp-1* peptide bind at the same site on DnaK. Schmid and co-workers have shown that peptide binding to DnaK can be quite fast. For example, at 25 °C the pp-1 peptide (Table 1) binds to DnaK with k_{on} and k_{off} values equal to 9400 M^{-1} s^{-1} and 4.0×10^{-3} s^{-1}, respectively. Under identical conditions, Cro* binds to DnaK with k_{on} and k_{off} values equal to 18 M^{-1} s^{-1} and 1.3×10^{-4} s^{-1} (Table 2), respectively. The pp-1 peptide contains several stretches of aliphatic residues interspersed with polar (Q, S) and positively charged (R) residues. The Cro peptide contains a small hydrophobic core (ITL) flanked on the N-terminal side by a polar and two charged residues (QER) and on the C-terminal side by two charged residues (KD) (Table 1). As stated above, solvation of the Cro peptide is another possible explanation for its slow binding to DnaK. We surmise that the pp-1 peptide, which contains both polar and charged residues, might also be solvated, yet pp-1 rapidly binds to DnaK. Solvation of the Cro peptide probably does not fully account for the difference in reactivities between the Cro and pp-1 peptides with DnaK. The difference in reactivities is more plausibly related to *charge* differences between the two peptides (Table 1). The unlabeled Cro peptide contains two positively charged residues and two negatively charged residues, thus the peptide is charged but neutral at pH 7. In contrast, the unlabeled pp-1 peptide, which is devoid of negatively charged residues, contains four positively charged residues at pH 7. Interestingly, according to Gragerov and co-workers (1994), *negatively* charged residues within the center of a short peptide inhibit or even eliminate binding to DnaK (Gragerov et al., 1994). We propose that this inhibition is a consequence of electrostatic repulsion between opposed negative charge(s) on a given peptide and negative charge(s) in the chaperone binding site. [Since DnaK has a very low isoelectric point (pI = 5.1; Zylicz & Georgopoulos, 1984), the protein is negatively charged at neutral pH. If the peptide binding site of DnaK contains one or more negatively charged residues, such charges could participate in the proposed transition-state destabilization.] With respect to the work described here, if electrostatic repulsions between the two negatively charged residues on the Cro* peptide and the putative negatively charged residues within the DnaK binding site inhibit DnaK−Cro* complex formation, the same electrostatic repulsions should promote rapid DnaK−Cro* complex dissociation. Yet, paradoxically, the rate of DnaK−Cro* complex dissociation is *31 times slower* than the rate of DnaK-pp1* complex dissociation (k_{off}[pp-1*]/k_{off}[Cro*] = 4.0×10^{-3} s^{-1}/1.3×10^{-4} s^{-1} = 31). One possibility is that, following the formation of a DnaK−Cro* encounter complex, elec-

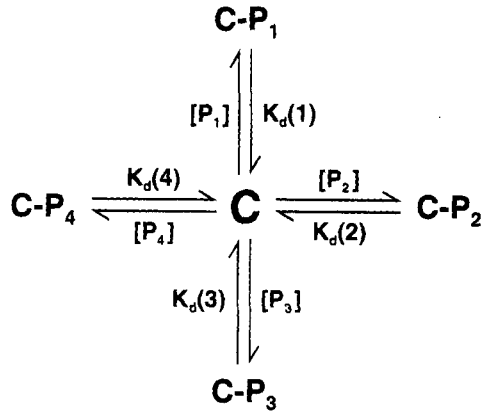

FIGURE 10: Hypothetical reactions between a molecular chaperone and four different peptides.

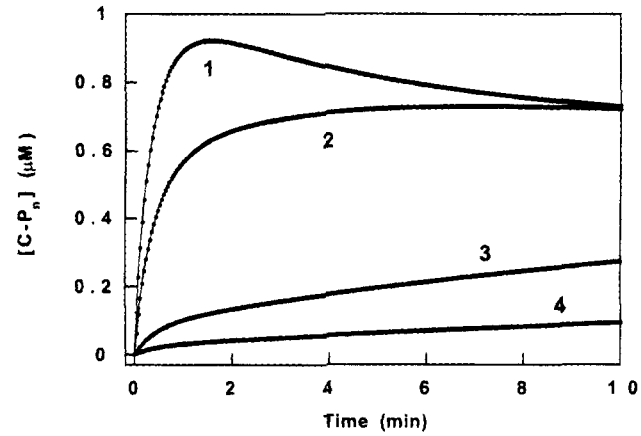

FIGURE 11: Simulated chaperone–peptide complex formation. The four parallel reversible reactions in Figure 10 were simulated with the following parameters: k_{off}/k_{on} values are 4.66×10^{-3} s^{-1}/14 000 M^{-1} s^{-1} (1); 2.33×10^{-3} s^{-1}/7000 M^{-1} s^{-1} (2); 3.3×10^{-4} s^{-1}/1000 M^{-1} s^{-1} (3); and 10^{-4} s^{-1}/300 M^{-1} s^{-1} (4); $[\text{chaperone}]_o = [P_1]_o = [P_2]_o = [P_3]_o = [P_4]_o = 2$ μM and $K_d(1-4) = 3.3 \times 10^{-7}$ M.

trostatic repulsions between the peptide and the chaperone are reduced via an intramolecular reaction. Such a reaction might involve a conformational change in the peptide or the chaperone or both.

In conclusion, the slow binding of the Cro* peptide to DnaK yields long-lived complexes. The low affinity of the Cro* peptide for DnaK is a consequence of a large kinetic barrier to binding. We suggest that the large kinetic barrier to binding is related to the two negatively charged residues within the Cro peptide. Further kinetic experiments employing Cro peptide analogs can test this idea.

APPENDIX

The four parallel reversible reactions depicted in Figure 10 represent the simultaneous presentation of several different peptides to a molecular chaperone. This is an idealized case since *in vivo* a chaperone may have ADP or ATP bound in the nucleotide binding site. We simulated the reactions to show that the "kinetic selection" of one peptide over another can occur at short times, even when several different peptides have the same affinity for the molecular chaperone. The reactions in Figure 10 were simulated by numerically integrating the rate equations associated with the forward and reverse reactions. The hypothetical peptides are referred to as P_1, P_2, P_3, and P_4. The simulation was conducted with the condition that each of the four sets of reversible reactions has the same equilibrium dissociation constant ($K_d = 0.33$ μM) but different values for k_{off} and k_{on}, as follows: $K_d(1) = k_{off}/k_{on} = 4.7 \times 10^{-3}$ $s^{-1}/1.4 \times 10^4$ M^{-1} s^{-1}; $K_d(2) = 2.3 \times 10^{-3}$ $s^{-1}/7.0 \times 10^3$ M^{-1} s^{-1}; $K_d(3) = 3.3 \times 10^{-4}$ $s^{-1}/1.0 \times 10^3$ M^{-1} s^{-1}; and $K_d(4) = 10^{-4}$ $s^{-1}/3.0 \times 10^2$ M^{-1} s^{-1}. The initial concentrations of chaperone and peptides are 2.0 μM. The simulated curves (Figure 11), which depict the kinetics of the approach to equilibrium for each of the four different hypothetical chaperone–peptide complexes (Figure 10), are characterized by the following features: (i) simulated curve 1 exhibits biphasic kinetics, with a rapid formation phase that is followed by a slow decay phase which ultimately reaches the equilibrium endpoint ($[\text{c-P}_1]_{eq} = 0.5$ μM) (not shown). The decay portion of the curve is due to the reduction in the number of c-P_1 complexes via competition with the other peptides; (ii) simulated formation curves (2–4) exhibit monophasic kinetics and gradually reach the equilibrium endpoint; (iii) the respective relaxation times for reactions **1–4** are 0.17, 0.32, 15.6, and 99 min; and (iv) although the four reactions have the same equilibrium endpoint, at short times there is a large disparity in the rates of formation and in the amounts of the different complexes; for example, at $t = 1$ min the ratio $[\text{c-P}_1]/[\text{c-P}_4] = 30$. This differential binding of hypothetical peptide P_1 over P_4 at short times is primarily due to the fact that $k_{on}(1)$ (1.4×10^4 M^{-1} s^{-1}) is larger than $k_{on}(4)$ (3.0×10^2 M^{-1} s^{-1}). On the basis of this simulation, when a molecular chaperone, such as DnaK, acts *in vivo*, the preferential binding of one substrate over another at short times is a consequence of disparate k_{on} values. The cofactor ATP and cochaperones GrpE and DnaJ probably function to modulate the activation energy barriers to chaperone–substrate complex formation (and dissociation).

ACKNOWLEDGMENT

We thank Dr. Roger McMacken for a gift of the RLM893 cells, which were originally established in the lab of Dr. Costas Georgopoulos; Dr. Mary Barkley for the use of the XL-A ultracentrifuge and Martha Juban and Gabriele Roithmeier for their expert technical assistance; and Drs. David Gross and Robert Smith for a critical reading of the manuscript.

REFERENCES

Becker, G., & Craig, E. A. (1994) *Eur. J. Biochem. 219*, 11–23.
Bevington, P. R. (1969) *Data Reduction and Error Analysis for the Physical Sciences*, pp 92–96, McGraw-Hill, New York.
Blond-Elguindi, S., Cwirla, S. E., Dower, W. J., Lipshutz, R. J., Sprang, S. R., Sambrook, J. F., & Gething, M. J. (1993) *Cell 75*, 717–728.
Brandts, J. R., & Kaplan, K. J. (1973) *Biochemistry 12*, 2011–2024.
Cegielska, A & Georgopoulos, C. (1989) *J. Biol. Chem. 264*, 21122–21130.
Espenson, J. H. (1981) *Chemical Kinetics and Reaction Mechanisms*, pp116–118, McGraw-Hill, New York.
Flaherty, K. M., DeLuca-Flaherty, C., & McKay, D. B. (1990) *Nature (London) 346*, 623–628.
Flynn, G. C., Chappell, T. G., & Rothman, J. E. (1989) *Science 245*, 385–390.
Flynn, G. C., Pohl, J., Flocco, M. T., & Rothman, J. E. (1991) *Nature 353*, 726–730.
Gallione, C. J., & Rose, J. K. (1983) *J. Virol. 46*, 162–169.

Georgopoulos, C., & Welch, W. J. (1993) *Annu. Rev. Cell. Biol. 9*, 601−634.
Gething, M.-J., & Sambrook, J. (1992) *Nature 355*, 33−45.
Gragerov, A., Zeng, L., Zhao, X., Burkholder, W., & Gottesman, M. E. (1994) *J. Mol. Biol. 235*, 848−854.
Haber, L. T., & Walker, G. C. (1991) *EMBO J. 10*, 2707−2715.
Haugland, R. P. (1992) *Handbook of Fluorescent Probes and Research Chemicals* (Karen D. Larison, Ed.) 5th ed., p 34, Molecular Probes, Inc., Eugene, OR.
Hendrick, J. P., & Hartl, F.-U. (1993) *Annu. Rev. Biochem. 62*, 349−384.
Hsiang, M. W., Cole, R. D., Takeda, Y., & Echols, H. (1977) *Nature 270*, 275−277.
Landry, S. J., Jordan, R., McMacken, R., & Gierasch, L. M. (1992) *Nature 355*, 455−457.
McCarty, J. S., & Walker, G. C. (1991) *Proc. Natl. Acad. Sci. U.S.A. 88*, 9513−9517.
McRorie, D. K., & Voelker, P. J. (1993) *Self-Associating Systems in the Analytical Ultracentrifuge*, p 15, Beckman Instruments, Inc.
Palleros, D. R., Welch, W. J., & Fink, A. L. (1991) *Proc. Natl. Acad. Sci. U.S.A. 88*, 5719−5723.
Palleros, D. R., Reid, K. L., Shi, L., Welch, W. J., & Fink, A. L. (1993a) *Nature 365*, 664−666.
Palleros, D. R., Reid, K. L., Shi, L., & Fink, A. L. (1993b) *FEBS Lett. 336*, 124−128.
Rippmann, F., Taylor, W. R., Rothbard, J. B., & Green, N. M. (1991) *EMBO J. 10*, 1053−1059.
Schmid, S. L., Braell, W. A., & Rothman, J. E. (1986) *J. Biol. Chem. 260*, 10057−10062.
Schmid, D., Baici, A., Gehring, H., & Christen, P. (1994) *Science 263*, 971−973.
Sherman, M. Y., & Goldberg, A .L. (1991) *J. Bacteriol. 173*, 7249−7256.
Wall, D., Zylicz, M., & Georgopoulos, C. (1995) *J. Biol. Chem. 270*, 2139−2144.
Zamyathin, A. A. (1984) *Annu. Rev. Biophys. 13*, 145−165.
Zuiderweg, E. R. P., Morshauser, R. C., Wang, H., & Flynn, G. (1995) *J. Cell. Biochem.* (Suppl.) *19B*, 207.
Zylicz, M., & Georgopoulos, C. (1984) *J. Biol. Chem. 259*, 8820−8825.

BI951706M